

This article was downloaded by:

On: 25 January 2011

Access details: *Access Details: Free Access*

Publisher *Taylor & Francis*

Informa Ltd Registered in England and Wales Registered Number: 1072954 Registered office: Mortimer House, 37-41 Mortimer Street, London W1T 3JH, UK



Separation Science and Technology

Publication details, including instructions for authors and subscription information:

<http://www.informaworld.com/smpp/title~content=t713708471>

Film Model Approximation for Particle-Diffusion-Controlled Binary Ion Exchange

Giorgio Carta^a; Alberto Cincotti^b; Giacomo Cao^b

^a DEPARTMENT OF CHEMICAL ENGINEERING, UNIVERSITY OF VIRGINIA, CHARLOTTESVILLE, VIRGINIA, USA ^b DIPARTIMENTO DI INGEGNERIA CHIMICA E MATERIALI, UNIVERSITA'

DEGLI STUDI DI CAGLIARI, CAGLIARI, ITALY

Online publication date: 01 November 1999

To cite this Article Carta, Giorgio , Cincotti, Alberto and Cao, Giacomo(1999) 'Film Model Approximation for Particle-Diffusion-Controlled Binary Ion Exchange', *Separation Science and Technology*, 34: 1, 1 – 16

To link to this Article: DOI: 10.1081/SS-100100632

URL: <http://dx.doi.org/10.1081/SS-100100632>

PLEASE SCROLL DOWN FOR ARTICLE

Full terms and conditions of use: <http://www.informaworld.com/terms-and-conditions-of-access.pdf>

This article may be used for research, teaching and private study purposes. Any substantial or systematic reproduction, re-distribution, re-selling, loan or sub-licensing, systematic supply or distribution in any form to anyone is expressly forbidden.

The publisher does not give any warranty express or implied or make any representation that the contents will be complete or accurate or up to date. The accuracy of any instructions, formulae and drug doses should be independently verified with primary sources. The publisher shall not be liable for any loss, actions, claims, proceedings, demand or costs or damages whatsoever or howsoever caused arising directly or indirectly in connection with or arising out of the use of this material.

Film Model Approximation for Particle-Diffusion-Controlled Binary Ion Exchange

GIORGIO CARTA*

DEPARTMENT OF CHEMICAL ENGINEERING
UNIVERSITY OF VIRGINIA
CHARLOTTESVILLE, VIRGINIA 22903-2442, USA

ALBERTO CINCOTTI and GIACOMO CAO

DIPARTIMENTO DI INGEGNERIA CHIMICA E MATERIALI
UNIVERSITA' DEGLI STUDI DI CAGLIARI
PIAZZA D'ARMI, I-09123 CAGLIARI, ITALY

ABSTRACT

A new rate expression for particle-diffusion-controlled ion exchange, based on an equivalent pseudosteady-state film resistance model, is developed. The rate expression approximates the electric field effects on intraparticle diffusion in spherical ion-exchangers. With regard to the prediction of batch exchange and column breakthrough curves for both irreversible and reversible processes, the model captures the essential traits of the coupled diffusion phenomenon described by the Nernst–Planck equation with results of accuracy comparable to that obtained when using the linear driving force approximation for systems with constant diffusivity. Numerical results for the exchange of two counterions of equal valence are presented as application examples for different mobility ratios and selectivity coefficients.

Key Words. Ion exchange; Mass transfer; Nernst–Planck model; Linear driving force approximation

INTRODUCTION

A quantitative description of adsorptive separation processes typically requires a representation of both equilibrium and rate phenomena. For example, when using particulate adsorbent media in a fixed bed, rate expressions de-

* To whom correspondence should be addressed.

scribing intraparticle diffusion are obtained by writing transient conservation equations in spherical coordinates for the particles. These equations are, in turn, coupled to overall transient balances for the column through boundary conditions at the particle–fluid interface, yielding a system of nonlinear partial differential equations in three independent variables: the column axis, the particle radius, and time. The resulting system of equations can be stiff because of the nonlinearity of the adsorption isotherm. Thus, it is often desirable to use simpler explicit expressions to represent the rate of interphase mass transfer. A popular choice is the so-called linear driving force (LDF) approximation, where the rate of interphase mass transfer is expressed as the product of a rate coefficient times a driving force written as a concentration difference. The LDF approximation was originally obtained by Glueckauf (1) for batch adsorption with a linear isotherm and a constant diffusivity. However, it is also often used to describe both batch and column adsorption processes even if the isotherm is nonlinear since it produces results which are typically qualitatively and often quantitatively correct (2).

The LDF approximation can be derived mathematically by assuming that the intraparticle concentration profile is parabolic (3). When the intraparticle diffusivity, \bar{D} , is constant, and the diffusion resistance in the adsorbed phase is dominant, the dimensionless intraparticle flux of an adsorbate species in a sorbent particle of radius r_p and capacity q_0 is given by

$$J^* = -\frac{\partial y}{\partial \rho} \quad (1)$$

where $J^* = r_p J / \bar{D} q_0$. y is the dimensionless solute concentration and ρ is the dimensionless radial coordinate. If the concentration profile inside the particle is assumed to be parabolic, we have (3):

$$\left(\frac{\partial y}{\partial \rho}\right)_{\rho=1} = 5(y^* - \bar{y}) \quad (2)$$

where \bar{y} is the average concentration in the sorbent particle and y^* is the equilibrium concentration at the particle surface. The following rate equation is obtained by combining Eq. (2) with an overall mass balance for the particle:

$$\frac{\partial \bar{y}}{\partial \tau} = 15(y^* - \bar{y}) \quad (3)$$

where $\tau = \bar{D}t/r_p^2$ is a dimensionless diffusion time.

For the exchange of two counterions A and B in an ion-exchange resin, the situation is further complicated by the electrical coupling of diffusion fluxes. When the mobilities of the exchanging ions are different, an electric field gradient is established during the exchange process giving rise to effec-



tive diffusivities that vary strongly with composition. In this case, for a counterion A of charge z_A , the equivalent dimensionless flux can be expressed by the Nernst–Planck equation (4):

$$J_A^* = -\frac{1}{\alpha} \left(\frac{\partial y_A}{\partial \rho} + z_A y_A \frac{\mathfrak{S}}{\mathfrak{R}T} \frac{\partial \phi}{\partial \rho} \right) \quad (4)$$

where $\alpha = \bar{D}_B/\bar{D}_A$ is the ratio of the self-diffusivities of the two counterions, y_A is the equivalent fraction in the exchanger phase, and ϕ is the electric potential. In this case the dimensionless flux is $J_A^* = r_p J_A / \bar{D}_B q_0$ where J_A is the equivalent ion flux and q_0 is the exchanger capacity. Assuming zero current ($J_A + J_B = 0$), and that the equivalent ion concentration inside the exchanger remains constant ($y_A + y_B = 1$), the electric field can be eliminated, yielding the result (5):

$$J_A^* = -\frac{(1 - \eta)y_A + \eta}{(1 - \eta\alpha)y_A + \eta\alpha} \frac{\partial y_A}{\partial \rho} \quad (5)$$

where $\eta = z_B/z_A$. As discussed by Helfferich (4), this equation shows that as y_A approaches unity, the controlling diffusivity becomes that of ion B. Conversely, as y_A approaches zero, the controlling diffusivity becomes that of ion A. Considering, for example, a batch system, the exchange process tends to proceed faster when the ion initially in the exchanger is the one with higher diffusivity than when the ion initially in the exchanger has lower diffusivity. Numerical results obtained with this equation are given by Helfferich and Plesset (5) and Plesset et al. (6) for exchange on a single particle, and by Kataoka et al. (7) for irreversible ion exchange in columns under constant-pattern conditions.

Approximations for these equations have been proposed by a few authors. Rendueles de la Vega et al. (8) proposed the use of a “corrected Fick diffusivity” for equivalent binary exchange ($\eta = 1$). In this approach the particle conservation equation (modeled assuming a slab geometry) is solved assuming a constant “corrected diffusivity” value. The latter value, in turn, is obtained by matching the numerical solution of the constant-diffusivity model to the numerical solution of the Nernst-Planck model (also for a slab geometry) in such a way as to obtain consistent results. Following a different approach, Melis et al. (9) developed an extension of the LDF approximation which does not require solving a partial differential equation. In this approach the intraparticle concentration profile is assumed to be parabolic and the electric potential gradient is calculated accordingly using Eq. (4) with the condition of zero electric current. For reversible binary exchange, the result can be expressed as



$$\frac{\partial \bar{y}_A}{\partial \tau} = 15 \frac{(1 - \eta)y_A^* + \eta}{(1 - \eta\alpha)y_A^* + \eta\alpha} (y_A^* - \bar{y}_A) \quad (6)$$

where the dimensionless time is $\tau = \bar{D}_B t / r_p^2$. Comparing Eq. (6) with Eqs. (3) and (5), we see that the term $[(1 - \eta)y_A^* + \eta] / [(1 - \eta\alpha)y_A^* + \eta\alpha]$ is a correction factor to the classical LDF approximation that depends on the exchanger composition, y_A^* , at the particle–fluid interface. Melis et al. (9) showed that this treatment, in general terms, provides a good approximation of the Nernst–Planck model for an experimental system characterized by a moderate selectivity coefficient and moderate values of α . Because of the assumption made in deriving the model, however, it is expected that this approximation is likely not adequate for ion-exchange systems where the intraparticle concentration profiles are far from parabolic. This occurs when the interfacial concentration y_A^* approaches unity, i.e., for irreversible (or very favorable) exchange, when the diffusivity ratio α is large (5, 6).

Thus, the objectives of this paper are twofold:

1. To develop a new approximate rate expression for binary ion exchange taking into account the electric field effect with validity for both small and large values of α .
2. To test this approximation with regard to the prediction of batch exchange and column breakthrough curves for both irreversible and reversible exchange in comparison with the results predicted by the Nernst–Planck model.

THEORETICAL DEVELOPMENT

Nernst–Planck Model

Dimensionless conservation equations for the Nernst–Planck model, assuming spherical particles and neglecting volume changes in the exchanger, can be written as

$$\frac{\partial y_A}{\partial \tau} = \frac{1}{\rho^2} \frac{\partial}{\partial \rho} \left[\rho^2 \frac{(1 - \eta)y_A + \eta}{(1 - \eta\alpha)y_A + \eta\alpha} \frac{\partial y_A}{\partial \rho} \right] \quad (7)$$

$$\rho = 0: \quad \frac{\partial y_A}{\partial \rho} = 0 \quad (7a)$$

$$\rho = 1: \quad y_A = y_A^* \quad (7b)$$

$$\tau = 0: \quad y_A = 0 \quad (7c)$$

$$\bar{y}_A = 3 \int_0^1 y_A \rho^2 d\rho \quad (7d)$$



These equations are related to overall balances which may be written as follows.

For a batch system:

$$\frac{dx_A}{d\tau} = -\lambda \frac{d\bar{y}_A}{d\tau} = -3\lambda \left[\frac{(1 - \eta)y_A + \eta}{(1 - \eta\alpha)y_A + \eta\alpha} \frac{\partial y_A}{\partial \rho} \right]_{\rho=1} \quad (8)$$

$$\tau = 0: x_A = x_A^0 \quad (8a)$$

where $\lambda = V_r q_0 / V_s C_0$.

For a column:

$$\frac{\partial \bar{y}_A}{\partial \tau'} + \frac{\partial x_A}{\partial \xi} = 0 \quad (9)$$

$$\frac{\partial \bar{y}_A}{\partial \tau'} = 3 \left[\frac{(1 - \eta)y_A + \eta}{(1 - \eta\alpha)y_A + \eta\alpha} \frac{\partial y_A}{\partial \rho} \right]_{\rho=1} \quad (9a)$$

$$\xi = 0: x_A = x_A^0 \quad (9b)$$

$$\tau' = 0: x_A = 0 \quad (9c)$$

where $\tau' = \tau - \xi/\Lambda$, $\xi = \Lambda \bar{D}_B z / w r_p^2$, and $\Lambda = (1 - \epsilon)q_0 / \epsilon C_0$.

The external mass transfer resistance is neglected in these equations. Thus, for an ideal system, y_A^* is related to the fluid-phase equivalent fraction in solution by the mass action law (4):

$$K \left(\frac{q_0}{C_0} \right)^{1/\eta - 1} = \frac{y_A^* (1 - x_A)^{1/\eta}}{(1 - y_A^*)^{1/\eta} x_A} \quad (10)$$

Dimensional forms of these equations can be found in Ref. 10. In general, a numerical solution is required unless $\eta = 1$ and $\alpha = 1$. This was obtained by discretizing the particle conservation equation in the ρ -direction using the finite difference scheme of Kataoka et al. (7). For the case of batch exchange, the resulting system of ordinary differential equations was integrated numerically together with Eq. (8) using subroutine DIVPAG in the IMSL library. For the case of exchange in a column, Eq. (9) was discretized in the axial direction by backward finite differences. In general this introduces numerical dispersion. However, in this case the number of axial discretization points was chosen sufficiently large so as not to affect significantly the accuracy of the numerical results. For the case of irreversible exchange, numerical approximations of the exact solution are given by Helfferich and coworkers



(5, 6) for a batch system and by Kataoka et al. (7) for constant-pattern breakthrough.

Film Model Approximation

To develop this approximation we note that if one assumes that the intraparticle mass transfer resistance is represented by pseudosteady-state diffusion through a hypothetical flat film of thickness $\delta = r_p/5$, a result mathematically equivalent to the Glueckauf LDF approximation (Eq. 3) is obtained for the case of a constant diffusivity system. Using the same representation for binary ion exchange, and expressing the flux with Eq. (5), yields the following equation and boundary conditions:

$$\frac{d}{d\rho} \left[\frac{(1 - \eta)y_A + \eta}{(1 - \eta\alpha)y_A + \eta\alpha} \frac{dy_A}{d\rho} \right] = 0 \quad (11)$$

$$\rho = 1 - \frac{1}{5}: \quad y_A = \bar{y}_A \quad (11a)$$

$$\rho = 1: \quad y_A = y_A^* \quad (11b)$$

Integrating Eq. (11) across the film and combining the result with an overall species balance for a spherical particle, the following film model approximation is obtained:

$$\frac{\partial \bar{y}_A}{\partial \tau} = 15 \left[\frac{1 - \eta}{1 - \eta\alpha} + \frac{\eta(1 - \alpha)}{1 - \eta\alpha} \frac{1}{\Delta} \right] (y_A^* - \bar{y}_A) \quad (12)$$

where

$$\Delta = \frac{(1 - \eta\alpha)(y_A^* - \bar{y}_A)}{\ln \left[\frac{(1 - \eta\alpha)y_A^* + \eta\alpha}{(1 - \eta\alpha)\bar{y}_A + \eta\alpha} \right]} \quad (12a)$$

The term in brackets in Eq. (12) represents a correction factor for the classical LDF approximation accounting for the effect of the electric field. When $\alpha = 1$ (equal diffusivities), Eq. (12) reduces to Eq. (3). Analytic solutions for batch adsorption and for constant pattern breakthrough can be found solving Eq. (8) or (9) with Eq. (12) for the case of irreversible exchange ($y_A^* = 1$) when $\eta = 1$, and are given below.

Film model solution for batch adsorption ($y_A^ = 1, \eta = 1$):*

$$15\tau = \ln \left\{ \frac{\ln(\alpha)}{\ln[(1 - \alpha)\bar{y}_A + \alpha]} \right\} + \sum_{k=1}^{\infty} \frac{\{\ln(\alpha)\}^k - \{\ln[(1 - \alpha)\bar{y}_A + \alpha]\}^k}{k \cdot k!} \quad (13)$$

Film model solution for irreversible constant pattern ($y_A^ = 1, \eta = 1$):*



$$15(\tau' - \xi) = -\ln\{\ln[(1 - \alpha)x_A + \alpha]\} - \sum_{k=1}^{\infty} \frac{\{\ln[(1 - \alpha)x_A + \alpha]\}^k}{k \cdot k!} + \gamma \quad (14)$$

In this case, for constant pattern $\bar{y}_A = x_A$. Equation (14) contains an integration constant γ which is obtained from the material balance condition (10):

$$\int_0^1 (\tau' - \xi) dx_A = 0 \quad (15)$$

This yields

$$\gamma = \int_0^1 \left\{ \ln\{\ln[(1 - \alpha)x_A + \alpha]\} + \sum_{k=1}^{\infty} \frac{\{\ln[(1 - \alpha)x_A + \alpha]\}^k}{k \cdot k!} \right\} dx_A \quad (16)$$

Other cases with $\eta \neq 1$ (or for reversible exchange) are easily handled numerically as discussed previously.

Equations (13) and (14) converge to the corresponding well-known results for constant diffusivity when $\alpha \rightarrow 1$; that is:

$$15\tau = -\ln(1 - \bar{y}_A) \quad (17)$$

for batch adsorption, and

$$15(\tau' - \xi) = -\ln(1 - x_A) - 1 \quad (18)$$

for constant pattern breakthrough (10). It should be noted that if the intraparticle concentration profile is assumed to be parabolic, results identical to Eqs. (17) and (18) are obtained independently of the value of α since that approximation yields $\bar{D} = \bar{D}_B = \text{constant}$ when $y_A^* = 1$.

RESULTS AND DISCUSSION

Numerical results comparing the exact Nernst–Planck model solution to the film model approximation are presented for different situations of potential practical interest for the case of equivalent exchange ($\eta = 1$): 1) irreversible batch exchange, 2) reversible batch exchange and 3) breakthrough behavior with both irreversible and reversible exchange. In each case, time is rendered dimensionless using the diffusivity of the leaving ion B. Curves calculated assuming a parabolic concentration profile inside the particle are also shown for comparison.



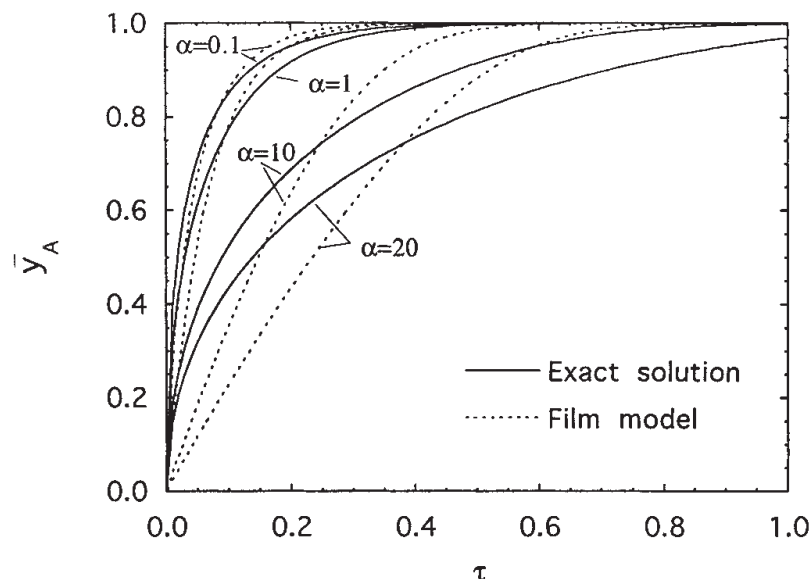


FIG. 1 Comparison of exact solution of Nernst–Planck model and film model approximation for irreversible batch exchange with $\eta = 1$. Resin initially in B-form.

Figure 1 shows results for the case of irreversible batch exchange with a constant surface concentration $y_A^* = 1$. For each value of α , the film model solution underestimates the exchange rate for short times and overestimates the rate for long times. This deficiency is characteristic of the LDF approximation. On the other hand, the effect of the electric field, i.e., the variation of the curves with α , is correctly predicted. In accordance with the exact Nernst–Planck solution, the rate is predicted to be faster when the faster ion is initially in the resin. In this case the assumption of a parabolic concentration profile would lead to a single curve independent of the value α and coincident with the curve shown for the film model with $\alpha = 1$.

Numerical results for reversible batch exchange are shown in Figs. 2 and 3 for values of the selectivity coefficient $K = 10$ and $K = 2$. Values of $x_A^0 = 0.7$ and $\lambda = 1$ were chosen for both cases. Both figures give the solution composition as a function of time. Curves calculated assuming that the concentration profile inside the particle is parabolic are also shown. For $K = 10$ (Fig. 2), when $\alpha < 1$, assuming that the intraparticle concentration profile is parabolic, tends to underestimate the exchange rate. The film model solution is closer to the exact Nernst–Planck model although, of course, it still underestimates the rate for short times and overestimates it for long times. For $\alpha = 1$, the film model and the solution obtained assuming a parabolic concentration profile coincide and both are in approximate agreement with the exact solution. As α become greater than 1, however, the solution obtained



assuming a parabolic concentration profile tends to overestimate the rate while the film model correctly predicts the general trend with regard to the effect of the electric field on the exchange rate. For values of $K = 2$ (Fig. 3), the equilibrium is less favorable and the interfacial concentration, y_A^* , attains lower values. In this case the intraparticle profiles retain a shape which is generally parabolic and, as a result, the solution obtained assuming a parabolic profile, as proposed by Melis et al. (9), compares favorably with the exact solution. The film model again provides an approximate prediction of the effect of the electric field and a qualitatively correct prediction of the shape of the x_A vs τ curves for each value of α .

A comparison of the different models for the case of irreversible constant pattern breakthrough is given in Fig. 4 for different values of α . In each case the effluent profiles are centered around the value $\tau' - \xi = 0$. However, the

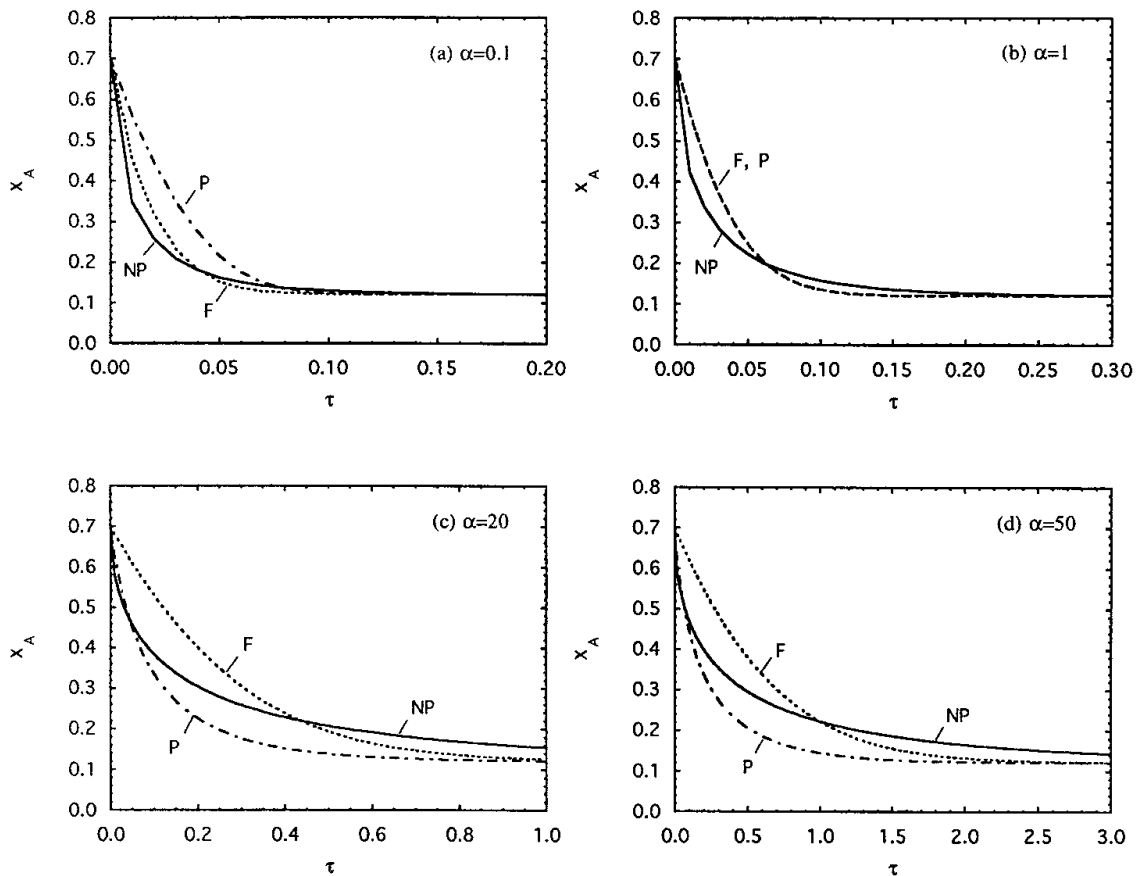


FIG. 2 Comparison of exact solution of Nernst-Planck model (NP), film model approximation (F), and solution obtained assuming a parabolic intraparticle concentration profile (P) for reversible batch exchange with $\eta = 1$, $\lambda = 1$, $x_A^0 = 0.7$, and $K = 10$. Resin initially in B-form.



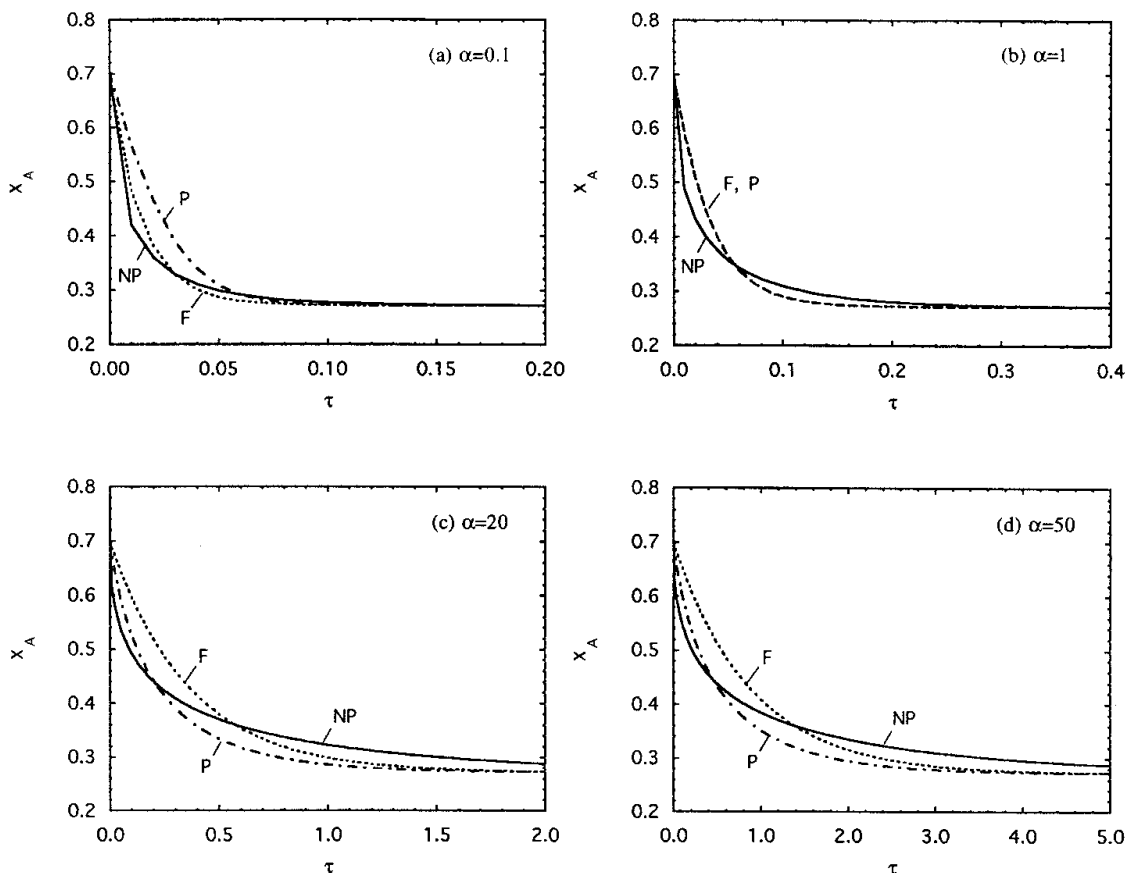


FIG. 3 Comparison of exact solution of Nernst-Planck model (NP), film model approximation (F), and solution obtained assuming a parabolic intraparticle concentration profile (P) for reversible batch exchange with $\eta = 1$, $\lambda = 1$, $x_A^0 = 0.7$, and $K = 2$. Resin initially in B-form.

slope decreases as the value of α increases. The solution obtained using the diffusivity of the ion initially present in the resin as the controlling diffusivity is also shown for comparison. This solution is obtained when the intraparticle concentration profile is assumed to be parabolic. The film model, while not reproducing the exact solution precisely everywhere, approximates the effect of the electric field for each value of α . Similar results are obtained for the case of reversible exchange. These results were obtained by numerical integration and are shown in Fig. 5 for $K = 10$ and in Fig. 6 for $K = 2$. For values of α of 1 or lower, the numerical results are nearly coincident independently of the value of K since, as noted by Kataoka et al. (7), the effect of the electric field is smaller when $\alpha \leq 1$. When the exchange is highly favorable, however, as in the case of $K = 10$, as α is increased the



solution obtained assuming a parabolic concentration profile inside the particles becomes progressively worse since it tends to predict a dominance of the diffusivity of the leaving ion. Thus, a steeper breakthrough curve is predicted by this model. The film model solution, on the other hand, continues to follow the breakthrough curve obtained from the Nernst–Planck model predicting quantitatively the effect of the electric field. As the exchange equilibrium becomes less favorable, as in the case of $K = 2$ shown in Fig. 6, the discrepancy between the different models becomes smaller. This occurs because the surface of the particle does not immediately attain a value of y_A^* approaching unity as in the case of irreversible or highly favorable exchange. Thus, in this case also the LDF correction factor obtained assuming a parabolic profile, as suggested by Melis et al. (9), provides a good approxi-

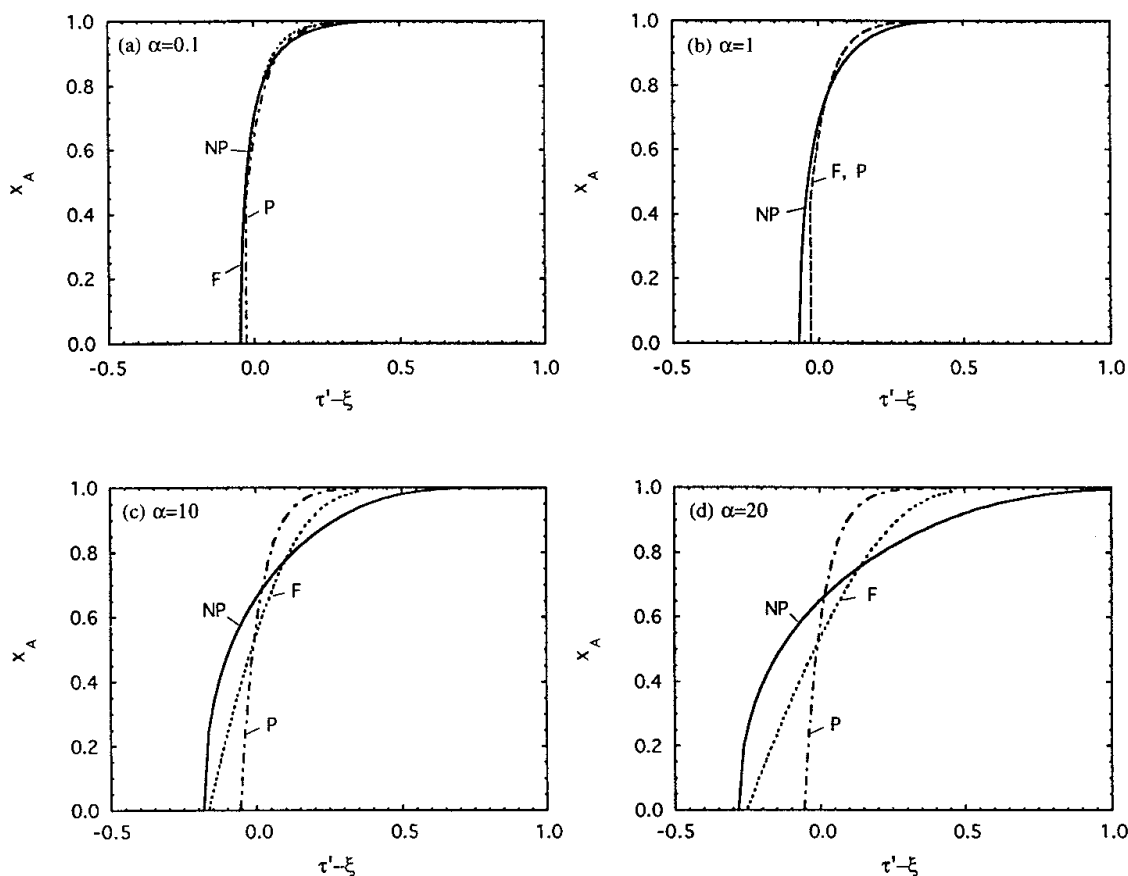


FIG. 4 Comparison of exact solution of Nernst–Planck model (NP), film model approximation (F), and solution obtained assuming a parabolic intraparticle concentration profile (P) for irreversible constant pattern breakthrough behavior with $\eta = 1$. Resin initially in B-form.



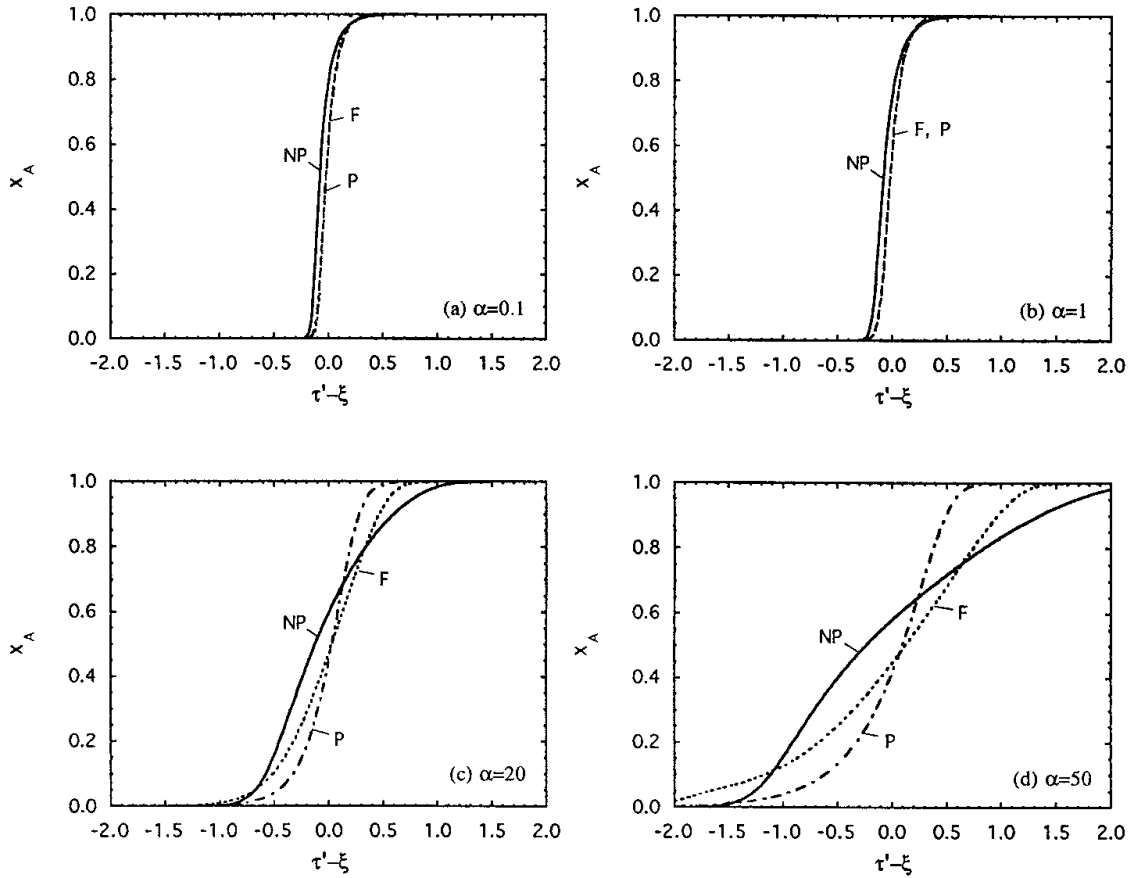


FIG. 5 Comparison of exact solution of Nernst-Planck model (NP), film model approximation (F), and solution obtained assuming a parabolic intraparticle concentration profile (P) for reversible breakthrough behavior with $\eta = 1$, $\Lambda = 1$, $\xi = 2$, $x_A^0 = 1$, and $K = 10$. Resin initially in B-form.

mation. It is worth noting that the film model appears to work well not only for constant-pattern or near constant-pattern conditions as shown in Fig. 4(a-d), Fig. 5(a-d), and in Fig. 6(a-c), but also for nonconstant-pattern conditions as shown in Fig. 6(d).

CONCLUSIONS

A rate expression for binary ion exchange, based on an equivalent pseudosteady-state film resistance model, approximates the effects of the electric field on intraparticle diffusion in spherical ion-exchanger particles. The model converges to the classical Glueckauf LDF approximation when the ions have equal diffusivity. When the diffusivities are different, however, the approximation contains a correction factor whose magnitude depends on the value



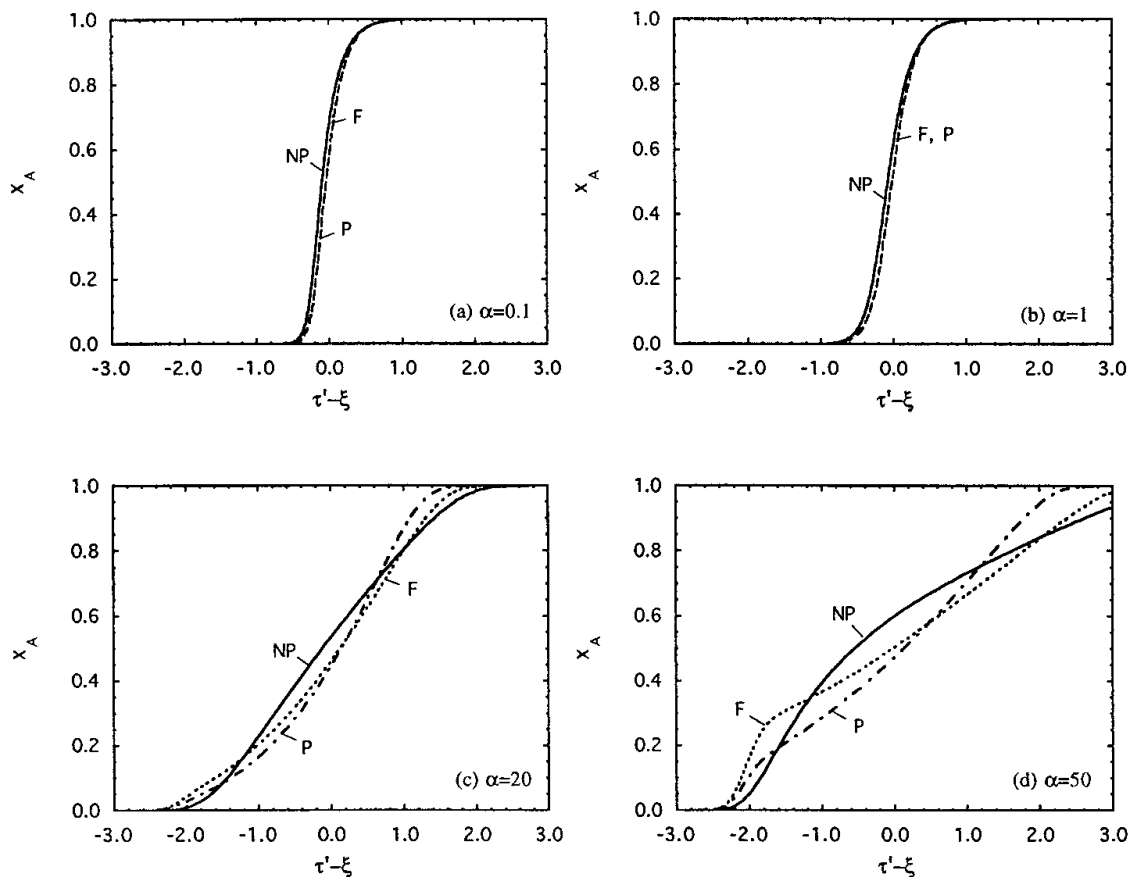


FIG. 6 Comparison of exact solution of Nernst–Planck model (NP), film model approximation (F), and solution obtained assuming a parabolic intraparticle concentration profile (P) for reversible breakthrough behavior with $\eta = 1$, $\Lambda = 1$, $\xi = 2$, $x_A^0 = 1$, and $K = 2$. Resin initially in B-form.

of the diffusivity ratio, α , and the charge ratio, η , of the two counterions. Calculated batch uptake curves and breakthrough curves obtained using this correction factor for equivalent exchange and both irreversible and reversible exchange are in good agreement with exact calculations based on the Nernst–Planck model for spherical particles. Thus, the equivalent film model appears to capture the essential traits of the coupled diffusion phenomenon in ion exchange, giving results of accuracy comparable to that obtained when using the LDF approximation for systems with constant diffusivity. The film model approximation should be useful for numerical calculations involving more complex equilibrium relationships and operating conditions where the intraparticle concentration profile cannot be approximated as a parabola. A disadvantage is that the extension to multicomponent systems is not straightforward, likely requiring the integration of a system of ODE's across the film.



NOMENCLATURE

C_i	concentration of species i (mol/L)
C_0	equivalent concentration (equiv/L)
\bar{D}	diffusivity of an adsorbate species in the adsorbed phase (cm ² /s)
\bar{D}_i	self-diffusivity of species i in the exchanger (cm ² /s)
\mathcal{F}	Faraday constant
J	molar flux of an adsorbate species in adsorbed phase (mol/cm ² ·s)
J_i	equivalent flux of species i (equiv/cm ² ·s)
J^*	dimensionless molar flux of an adsorbate species in adsorbed phase (= $r_p J / \bar{D} q_0$)
J_i^*	dimensionless equivalent flux of species i (= $r_p J_i / \bar{D}_B q_0$)
K	selectivity coefficient for exchange reaction
q_i	concentration of species i in adsorbed or exchanger phase (mol/L)
q_0	adsorbent or exchanger capacity (mol/L or equiv/L)
r	particle radial coordinate (cm)
r_p	particle radius (cm)
\mathcal{R}	ideal gas constant
t	time (s)
T	temperature (K)
v	fluid velocity (cm/s)
V_r	exchanger volume (L)
V_s	solution volume (L)
z	bed length or axial coordinate (cm)
z_i	charge of species i
x_i	equivalent fraction of species i in solution (= $z_i C_i / C_0$)
x_i^0	initial or feed equivalent fraction of species i in solution
y_i	equivalent fraction of species i in exchanger phase (= $z_i q_i / q_0$)
\bar{y}_i	average equivalent fraction of species i in exchanger phase
y_i^*	equilibrium equivalent fraction of species i in exchanger phase at particle surface

Greek Letters

α	diffusivity ratio (= \bar{D}_B / \bar{D}_A)
δ	film thickness (cm)
ϵ	bed void fraction
ϕ	electric potential
η	charge ratio (= z_B / z_A)
λ	capacity factor for batch exchange (= $V_r q_0 / V_s C_0$)
Λ	bed capacity factor [= $(1 - \epsilon) q_0 / \epsilon C_0$]
ρ	dimensionless radial coordinate (= r / r_p)



- τ dimensionless time ($= \bar{D}_B t / r_p^2$)
 τ' dimensionless time ($= \tau - \xi / \Lambda$)
 ξ dimensionless axial coordinate ($= \bar{D}_B (1 - \epsilon) q_0 z / r_p^2 \epsilon C_0 V$)

ACKNOWLEDGMENTS

One of the authors, G.C., was a Visiting Professor at the Università di Cagliari during completion of this work. The hospitality of the Dipartimento di Ingegneria Chimica e Materiali is gratefully acknowledged.

REFERENCES

1. E. Glueckauf, *Trans. Faraday Soc.*, 51, 1540 (1955).
2. D. M. Ruthven, *Principles of Adsorption and Adsorption Processes*, Wiley, New York, NY, 1984.
3. C. M. Liaw, J. S. P. Wang, R. A. Greenkorn, and K. C. Chao, *AIChE J.*, 25, 376 (1979).
4. F. Helfferich, *Ion Exchange*, McGraw-Hill, New York, NY, 1962.
5. F. Helfferich and M. S. Plesset, *J. Chem. Phys.*, 28, 418 (1958).
6. M. S. Plesset, F. Helfferich, and J. N. Franklin, *Ibid.*, 29, 1064 (1958).
7. T. Kataoka, H. Yoshida, and Y. Ozasa, *J. Chem. Eng. Jpn.*, 10, 385 (1977).
8. M. Rendueles de la Vega, J. M. Loureiro, and A. E. Rodrigues, *Chem. Eng. J.*, 61, 123 (1996).
9. S. Melis, J. Markos, G. Cao, and M. Morbidelli, *Ind. Eng. Chem. Res.*, 35, 3629 (1996).
10. M. D. LeVan, G. Carta, and C. M. Yon, "Adsorption and Ion Exchange," in *Perry's Chemical Engineers Handbook*, 7th ed. (Ch. 16), McGraw-Hill, New York, NY, 1997.

Received by editor January 14, 1998

Revision received May 1998



Request Permission or Order Reprints Instantly!

Interested in copying and sharing this article? In most cases, U.S. Copyright Law requires that you get permission from the article's rightsholder before using copyrighted content.

All information and materials found in this article, including but not limited to text, trademarks, patents, logos, graphics and images (the "Materials"), are the copyrighted works and other forms of intellectual property of Marcel Dekker, Inc., or its licensors. All rights not expressly granted are reserved.

Get permission to lawfully reproduce and distribute the Materials or order reprints quickly and painlessly. Simply click on the "Request Permission/Reprints Here" link below and follow the instructions. Visit the [U.S. Copyright Office](#) for information on Fair Use limitations of U.S. copyright law. Please refer to The Association of American Publishers' (AAP) website for guidelines on [Fair Use in the Classroom](#).

The Materials are for your personal use only and cannot be reformatted, reposted, resold or distributed by electronic means or otherwise without permission from Marcel Dekker, Inc. Marcel Dekker, Inc. grants you the limited right to display the Materials only on your personal computer or personal wireless device, and to copy and download single copies of such Materials provided that any copyright, trademark or other notice appearing on such Materials is also retained by, displayed, copied or downloaded as part of the Materials and is not removed or obscured, and provided you do not edit, modify, alter or enhance the Materials. Please refer to our [Website User Agreement](#) for more details.

[Order now!](#)

Reprints of this article can also be ordered at

<http://www.dekker.com/servlet/product/DOI/101081SS100100632>